CYBERNETICS AND PHYSICS, VOL. 1, NO. 1, 2012 , 58–66

IN-PHASE AND ANTI-PHASE SYNCHRONIZATION OF OSCILLATORS WITH HUYGENS' COUPLING

Jonatan Peña-Ramírez
Dep. of Mech. Engineering
Eindhoven University of
Technology, Netherlands
J.Pena@tue.nl

Rob H.B. Fey
Dep. of Mech. Engineering
Eindhoven University of
Technology, Netherlands
R.H.B.Fey@tue.nl

H. Nijmeijer
Dep. of Mech. Engineering
Eindhoven University of
Technology, Netherlands
H.Nijmeijer@tue.nl

Abstract
In this experimental study, the synchronized motion observed in pairs of nonlinear oscillators coupled through a suspended rigid bar, is analyzed. In particular, the dynamics of two mass-spring-damper oscillators and the dynamics of two van der Pol oscillators are considered. It is shown that in both cases, the oscillators may exhibit in-phase and anti-phase synchronization. The experiments are executed in an experimental setup, consisting of two mass-spring-damper-oscillators coupled through a suspended rigid bar. A relation between the obtained results and Huygens' experiment of pendulum clocks is emphasized.

Key words
Synchronization, Huygens' coupling, nonlinear oscillators, dynamics.

1 Introduction

Synchronization of oscillating objects or bodies seems to happen in a natural way, i.e. if the bodies are programmed in such a way that a weak interaction between them will result in an adjustment of their rhythms. Several examples can be found in literature [Strogatz, 2003; Pikovsky, Rosenblum, and Kurths, 2001].

Probably the earliest writing on inanimate synchronization is due to the Dutch scientist Christiaan Huygens (1629-1695), who discovered that two pendulum clocks hanging from a common support (a wooden bar supported by two chairs), after some transient behaviour, kept in pace relative to each other such that the two pendulums always swing together (in opposite motion) and never varied. Huygens called this "sympathy of two clocks" [Pikovsky, Rosenblum, and Kurths, 2001; Huygens, 1660].

Two other classical examples related to the synchronization phenomenon are due to John William Strutt (Lord Rayleigh, 1842-1919) and Balthasar van der Pol (1889-1959). Rayleigh discovered that two organ tubes may produce a synchronized sound provided the outlets are close to each other [Rayleigh, 1945], and van der Pol studied the synchronization phenomenon of (harmonic and nonharmonic) electric oscillations [van der Pol, 1920].

Around 1948, the occurrence of spontaneous synchronization was also addressed by Russian scientists, who observed that two unbalanced rotors mounted on the same vibrating support structure and driven by asynchronous motors may synchronize under certain conditions [Blekhman, 1988].

Nowadays, there exists a large number of studies addressing the phenomenon of synchronization in several fields like biology, chemistry, physics, and engineering. Several couplings/controllers have been developed in order to achieve synchronized motion in a pair (or a network) of oscillators. Although Huygens' experiment has been revisited several times [Bennett et al., 2002; Pantaleone, 2002; Oud, Nijmeijer, and Pogromsky, 2006; Czolczynski et al., 2011], the use of Huygens' coupling to synchronize two *arbitrary* second order nonlinear oscillators has not been studied extensively.

This paper addresses the problem of synchronizing pairs of (identical) nonlinear oscillators with Huygens' coupling. The original Huygens system is slightly modified in the sense that each pendulum clock is replaced by an arbitrary second order nonlinear oscillator. The coupling bar, i.e. Huygens' coupling, will be considered as the key element in the occurrence of synchronization. In particular, it is shown that the mass of the coupling bar determines the eventual synchronized behaviour in the oscillators, namely in-phase or anti-phase synchronization. Three examples are considered: pairs of mass-spring-damper oscillators and a pair of van der Pol oscillators. For the case of mass-spring-damper oscillators, two different controllers are considered, namely a state dependent discontinuous con-

troller and an energy-based controller. The purpose of these controllers is to sustain the oscillations in the system. It is shown that the synchronized motion in the oscillators is independent of the kind of controller used to maintain the oscillations. Ultimately, it is experimentally demonstrated that two nonlinear oscillators may synchronize without the influence of an explicit control action, provided that the oscillators are linked through Huygens' coupling.

An experimental platform consisting of a suspended (controllable) rigid bar (in Huygens' example the wooden bar on two wooden chairs) and two (controllable) mass-spring-damper oscillators (the pendulum clocks in Huygens' case) is used in the experimental analysis. In fact, this setup has the potential that its dynamical behaviour can be adjusted. This is possible due to the fact that the oscillators and the coupling bar can be actuated independently, then by using feedback, it is possible to enforce specific desirable oscillators' dynamics and likewise it is possible to modify, if desired, the behaviour of the coupling bar.

The outline of the paper is as follows. First, a generalized (and simplified) version of Huygens' system, corresponding to our experimental setup is described in Section 2. Next, in Section 3, the in-phase and anti-phase synchronization of mass-spring-damper oscillators with two different types of controllers is investigated. In Section 4, the dynamics of the experimental setup is modified in order to mimic two coupled van der Pol oscillators. In-phase and anti-phase synchronization is discussed. Finally, a discussion of obtained results and conclusions are formulated in Sections 5.

2 Experimental setup and model description

In the original setup of pendulum clocks used by Huygens in his discovery of synchronization, the coupling between the clocks was a wooden bar supported by two chairs. In its simplest form, the wooden bar at the top of two chairs can be modeled by a single degree of freedom (dof) suspended rigid bar. The pendulum clocks can be replaced by two damped/driven pendula [Pogromsky, Belykh, and Nijmeijer, 2003].

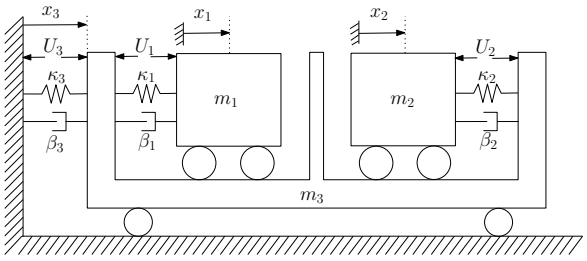

Figure 1. Schematic representation of the setup.

A further simplification of the Huygens system is the schematic model depicted in Figure 1. In this model, the pendulum clocks are now replaced by two (actuated) mass-spring-damper oscillators and the wooden bar at the top of two chairs is again modeled by a single dof suspended rigid bar. Note that in this model rotational angles are replaced by translational displacements. The control inputs U_1, U_2 of the two oscillators can be used to guarantee steady-state oscillations and/or to modify the inherent dynamic properties of the system, like mass, stiffness, and damping, in a desired way.

The idealized -i.e. assuming that no friction is present- equations of motion of the system of Figure 1 are

$$\begin{aligned}
\ddot{x}_1 &= -\omega_1^2(x_1 - x_3) - 2\zeta_1\omega_1(\dot{x}_1 - \dot{x}_3) + \frac{1}{m_1}U_1 \\
\ddot{x}_2 &= -\omega_2^2(x_2 - x_3) - 2\zeta_2\omega_2(\dot{x}_2 - \dot{x}_3) + \frac{1}{m_2}U_2 \qquad (1) \\
\ddot{x}_3 &= -\sum_{i=1}^{2}\mu_i\left(\ddot{x}_1 + \ddot{x}_2\right) - \omega_3^2 x_3 - 2\zeta_3 w_3\dot{x}_3 + \frac{1}{m_3}U_3,
\end{aligned}$$

where the mass of each subsystem is given by m_i $(i = 1, 2, 3)$, $\omega_i = \sqrt{\frac{\kappa_i}{m_i}}$ $[rad\ s^{-1}]$, $\zeta_i = \frac{\beta_i}{2\omega_i m_i}$ $[-]$ are respectively the angular eigenfrequency and dimensionless damping coefficient present in subsystem i $(i = 1, 2, 3)$, and the coupling strengths are denoted by $\mu_i = \frac{m_i}{m_3}$ $(i = 1, 2)$. These parameters are given in Table 2. The electric actuator force for subsystem i is denoted as U_i. The stiffness and damping characteristics present in the system are assumed to be linear with constants coefficients $\kappa_i, \beta_i \in \mathbb{R}^+$. Finally, $x_i \in \mathbb{R}$ $(i = 1, 2, 3)$, are the displacements of the two oscillators and the coupling bar respectively.

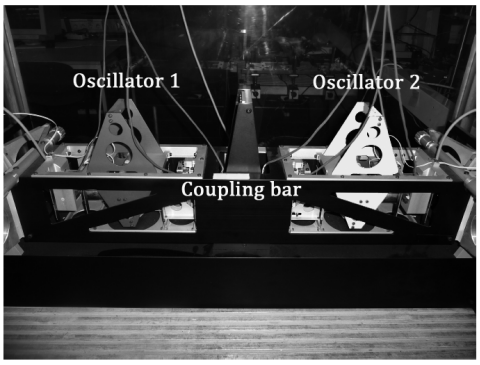

Figure 2. Photo of the experimental setup at TU/e.

As a matter of fact, the diagram of Figure 1 schematically describes the experimental setup of Figure 2, which has been constructed in order to study synchronization of coupled oscillators in general. By means of feedback control, it is possible to adjust the dynamical properties of the setup. Obviously, this opens the possibility of analyzing synchronous behaviour in a wide

variety of dynamical systems. This experimental platform can be used to validate (robustness of) theoretical findings. Moreover, the obtained experimental results may indicate new and interesting directions for research. A detailed description of the setup is presented in a previous paper [Pena-Ramirez, Fey, and Nijmeijer, 2011].

3 Phase synchronization of pairs of mass-spring-damper oscillators with two different types of controllers

In this section, the limit behaviour of mass-spring-damper oscillators with two different types of controllers and with Huygens' coupling is analyzed. Due to the damping in the system, it is clear that a control signal should be designed such that the oscillations do not damp out. The need of having a control input can be linked to Huygens' case, where the pendulum clocks are driven by an escapement mechanism in order to keep the clocks running. First, the oscillations in each oscillator are sustained by a state dependent discontinuous controller and secondly, an energy-based controller is used. As will be shown, the controllers are such that the oscillators in fact become nonlinear and self-sustained. It is demonstrated that the kind of controller used to sustain the oscillations in the oscillators seems to be irrelevant in the synchronized motion of the system. It will be emphasized that the spontaneous synchronized motion in the oscillators is indeed due to the interaction of the oscillators through the suspended rigid bar.

3.1 State dependent discontinuous controller

The original escapement mechanism of a pendulum clock "kicks" the pendulum each time a certain threshold angle is achieved. In other words, energy is "pumped" into the system. However, the modeling of this escapement mechanism is far from trivial and some simplifications should be made. In analogy to this escapement, the following state dependent controllers are implemented in system (1) such that the oscillations do not damp out

$$U_i = -m_i\alpha_i\dot{x}_i \text{sign}(|x_i| - x_{ref}), \quad i = 1, 2, \quad (2)$$
$$U_3 = 0, \quad (3)$$

where $\alpha_i \in \mathbb{R}^+$ defines the amplitude of the force U_i, the constant $x_{ref} \in \mathbb{R}^+$ represents a threshold displacement value and

$$\text{sign}(x) = \begin{cases} 1 \text{ if } x > 0, \\ 0 \text{ if } x = 0, \\ -1 \text{ if } x < 0. \end{cases} \quad (4)$$

U_3 is taken to be zero because we want the bar to oscillate freely. Moreover, it is clear that the controllers (2)-(3) convert system (1) into a discontinuous piecewise-linear system. Additionally, (2) assures that in steady-state, system (1) will exhibit stable oscillations.

3.1.1 Analysis of the anti-phase synchronization

Consider the simplified case $m = m_1 = m_2$, $\omega = \omega_1 = \omega_2$, $\zeta = \zeta_1 = \zeta_2$, and $\alpha = \alpha_1 = \alpha_2$. The analysis continues under the assumption that $|x_1(t)| < x_{ref}$ and $|x_2(t)| < x_{ref}$, $\forall t \in [0, t_1]$, for some $t_1 > 0$ [Dilão, 2009]. This implies that (1) is transformed to the linear system

$$\begin{aligned} \ddot{x}_1 &= -\omega^2(x_1 - x_3) - 2\zeta\omega(\dot{x}_1 - \dot{x}_3) + \alpha\dot{x}_1 \\ \ddot{x}_2 &= -\omega^2(x_2 - x_3) - 2\zeta\omega(\dot{x}_2 - \dot{x}_3) + \alpha\dot{x}_2 \\ \ddot{x}_3 &= -\frac{m}{m_3}(\ddot{x}_1 + \ddot{x}_2) - \omega_3^2 x_3 - 2\zeta_3\omega_3\dot{x}_3. \end{aligned} \quad (5)$$

The situation where $\alpha > 2\zeta\omega$ will be considered, so that the trivial solution $x_1 = x_2 = x_3 = 0$ of system (5) is unstable. If system (5) synchronizes in anti-phase, then all trajectories converge to the anti-phase manifold $M_{anti} := \{(x_1, \dot{x}_1) = (-x_2, -\dot{x}_2),\ x_3 = \dot{x}_3 = 0\}$. Therefore, it is quite natural to define anti-phase synchronization errors and their time derivatives as

$$\begin{aligned} e_1 &= x_1 + x_2, \quad & \dot{e}_1 &= \dot{x}_1 + \dot{x}_2, \\ e_2 &= x_3, & \dot{e}_2 &= \dot{x}_3. \end{aligned} \quad (6)$$

Writing the error dynamics as a set of first order differential equations yields

$$\frac{\mathrm{d}}{\mathrm{d}t}\begin{bmatrix} e_1 \\ \dot{e}_1 \\ e_2 \\ \dot{e}_2 \end{bmatrix} = \underbrace{\begin{bmatrix} 0 & 1 & 0 & 0 \\ -\omega^2 & -(2\zeta\omega - \alpha) & 2\omega^2 & 4\zeta\omega \\ 0 & 0 & 0 & 1 \\ \frac{m\omega^2}{m_3} & \left(\frac{2\zeta\omega m}{m_3} - \frac{\alpha m}{m_3}\right) & a & b \end{bmatrix}}_{A} \begin{bmatrix} e_1 \\ \dot{e}_1 \\ e_2 \\ \dot{e}_2 \end{bmatrix}, \quad (7)$$

where $a = -\left(\frac{2\omega^2 m}{m_3} + \omega_3^2\right)$ and $b = -\left(\frac{4\zeta\omega m}{m_3} + 2\zeta_3\omega_3\right)$. It is well known from stability theory for linear systems that (7) is asymptotically stable, if and only if the real parts of the eigenvalues of matrix A are negative. Then, the following proposition holds.

Proposition 1. *System (5) will converge to the set where $x_1(t) = -x_2(t)$, $\dot{x}_1(t) = -\dot{x}_2(t)$, $x_3(t) = 0$, $\dot{x}_3(t) = 0$ provided that all roots of the characteristic polynomial:*

$$\begin{aligned} p(\lambda) = \lambda^4 + (2\zeta\omega + \alpha + 2\zeta_3\omega_3 + 4\zeta\omega\frac{m}{m_3})\lambda^3 \\ +(4\zeta\omega\zeta_3\omega_3 + 2\alpha\zeta_3\omega_3 + \omega_3^2 + \omega^2 + 2\frac{m}{m_3}\omega^2)\lambda^2 \\ +(\alpha\omega_3^2 + 2\zeta\omega\omega_3^2 + 2\omega^2\zeta_3 w_3)\lambda + \omega^2\omega_3^2 \end{aligned}$$

all have negative real parts.

For a given set of fixed parameters $m, \omega, \omega_3, \alpha, \zeta$, and ζ_3, the only way to modify the roots of the characteristic polynomial (8) is by varying m_3.

Remark 1. *When the oscillators reach anti-phase synchronization - i.e. $x_1 = -x_2$, and $\dot{x}_1 = -\dot{x}_2$ - the displacement of the bar converges to zero, while for the in-phase motion, where $x_1 = x_2$, and $\dot{x}_1 = \dot{x}_2$, the displacement of the bar converges to a small periodic motion. Therefore, it is quite natural to think that a relatively light bar will facilitate the in-phase synchronization and for a relatively heavy bar, the anti-phase synchronization seems more feasible. Consequently, for relatively small values of the mass m_3, in comparison with the mass of the oscillators, i.e. large μ, in-phase synchronization is expected. For larger values of the mass m_3, in comparison with the masses of the oscillators, i.e. small μ, anti-phase synchronization is expected. For a really heavy bar, i.e. $\mu \to 0$, no coupling behaviour is expected. This reasoning can be linked to Huygens' situation, where the coupling strength μ (the ratio of clocks masses to wooden bar mass) is small due to the fact that Huygens had placed some extra weight (around 100 pounds) in the cases of the clocks in order to keep them upright in stormy seas. In such situations (small μ), Huygens always observed anti-phase synchronization [Bennett et al., 2002].*

Remark 2. *Proposition 1 cannot be directly linked to the original system (1)-(2). Therefore, the most that can be said is that in the interval of m_3 where Proposition 1 holds, anti-phase synchronization in system (1)-(2) is likely to occur.*

Notice that the analytical study of in-phase synchronization turns out to be more difficult. This is partly because the assumptions $|x_1(t)| < x_{ref}$, $|x_2(t)| < x_{ref}$ $\forall t \in [0, t_1]$ for some $t_1 > 0$ and $\alpha > 2\zeta\omega$ used in Proposition 1, yield a linear error system (similar to (7)), which is *independent* of m_3 and moreover, the obtained matrix A is not Hurwitz. It seems that the approach used for analyzing the anti-phase motion does not lead to insight in the stability of the in-phase synchronized behaviour. Therefore, a complete nonlinear stability analysis should be carried out in order to prove the stability of the in-phase synchronized motion. This problem is beyond the scope of this article and needs further research.

3.2 Energy-based escapement mechanism

As discussed before, due to the damping present in system (1), it is necessary to introduce a control input in order to have sustained oscillations in steady-state. In this section, it is assumed that the resupply of energy into the system is provided by the following energy-based controller

$$U_i = -\lambda \left(H_i - H^*\right) \dot{x}_i, \qquad i = 1, 2, \tag{8}$$

where $\lambda \in \mathbb{R}^+$, $H^* = \frac{1}{2}\kappa x_{ref}^2$ is a reference energy level, x_{ref} is the reference amplitude, $\kappa = \kappa_1, \kappa_2$, and H_i is the Hamiltonian for the uncoupled and unforced oscillator i, which is defined as

$$H_i = \frac{1}{2} m_i \dot{x}_i^2 + \frac{1}{2}\kappa_i x_i^2, \qquad i = 1, 2. \tag{9}$$

Furthermore, each Hamiltonian satisfies the relation

$$\dot{H}_i = -\lambda (H_i - H^*)\dot{x}_i^2, \quad i = 1, 2. \tag{10}$$

From this equation, it can be concluded that there exist values of λ such that the displacement of each oscillator in (1) converges to a periodic solution, which corresponds to the motion of the uncoupled oscillator with energy equal to H^*.

Furthermore, it should be noticed that system (5) with input (8) has at least two invariant sets, namely the anti-phase invariant set $\Omega_1 := \{x_1 = -x_2, \dot{x}_1 = -\dot{x}_2, x_3 = 0, \dot{x}_3 = 0\}$ and the in-phase invariant set $\Omega_2 := \{x_1 = x_2, \dot{x}_1 = \dot{x}_2\}$.

The local stability analysis for the set Ω_1 can be performed by linearizing system (5) with input (8) around the set $H_1(x_1, \dot{x}_1) = H_2(x_2, \dot{x}_2) = H^*$. This yields

$$\begin{aligned} \ddot{x}_1 + \ddot{x}_2 &= -\omega^2(x_1 + x_2) - 2\zeta\omega(\dot{x}_1 + \dot{x}_2) \\ &\quad +2\omega^2 x_3 + 4\zeta\omega\dot{x}_3 \\ \ddot{x}_3 &= -\frac{m}{m_3}(\ddot{x}_1 + \ddot{x}_2) - \omega_3^2 x_3 - 2\zeta_3\omega_3\dot{x}_3. \end{aligned} \tag{11}$$

This set of equations coincides with (7) with $\alpha = 0$, i.e. it can be rewritten as

$$\frac{\mathrm{d}}{\mathrm{d}t}\begin{bmatrix} e_1 \\ \dot{e}_1 \\ e_2 \\ \dot{e}_2 \end{bmatrix} = \underbrace{\begin{bmatrix} 0 & 1 & 0 & 0 \\ -\omega^2 & -2\zeta\omega & 2\omega^2 & 4\zeta\omega \\ 0 & 0 & 0 & 1 \\ \frac{m\omega^2}{m_3} & \left(\frac{2\zeta\omega m}{m_3}\right) & a & b \end{bmatrix}}_{A} \begin{bmatrix} e_1 \\ \dot{e}_1 \\ e_2 \\ \dot{e}_2 \end{bmatrix}. \tag{12}$$

Since A is Hurwitz for any combination of positive parameter values, the set Ω_1 is locally stable. Therefore, the anti-phase synchronous motion of the oscillators is locally asymptotically stable.

3.3 Experimental results

In this subsection, experimental results are presented in order to show different synchronizing limit behaviours. First, the discontinuous controller (2) is applied to system (1). All experiments are performed assuming the constant parameter values presented in Table 1. Only m_3, the mass of the coupling bar, is varied. Two experiments are presented: one corresponding to a light coupling bar, where in-phase sync is observed, and a second experiment corresponding to a heavier bar, where the conditions of Proposition 1 are fulfilled

	Osc. 1	Osc. 2	Coupling bar
$\kappa_i \left[\frac{\mathrm{N}}{\mathrm{m}}\right]$	37.108	37.108	388.71
$\beta_i \left[\frac{\mathrm{Ns}}{\mathrm{m}}\right]$	2.1378	2.1378	3.2656
m_i [kg]	0.210	0.210	[4.1-8.818]

Table 1. Parameters values for the experiments.

for $t \in [0, t_1]$ and anti-phase synchronization of the nonlinear system is therefore likely to occur and actually does occur. In all experiments, the phase difference (denoted Δ_{phase}) between the two oscillators is computed [Bennett et al., 2002].

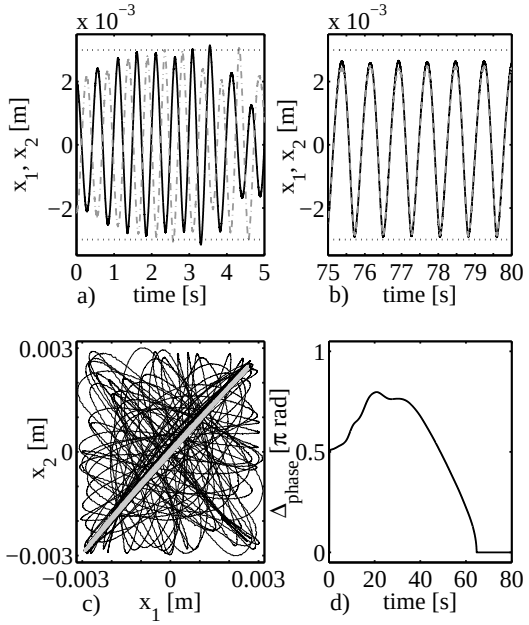

Figure 3. Experimental results: the oscillators synchronize in-phase (in figures a) and b) solid line: x_1, dashed-dotted line: x_2).

In the first experiment, no extra mass is added to the coupling bar, hence $m_3 = 4.1$ [kg]. The oscillators are released from the initial conditions $x_1(0) = 1.97$ $[mm]$, $\dot{x}_1(0) = 0$, $x_2(0) = -2.13$ $[mm]$, $\dot{x}_2(0) = 0$, and $x_3(0) = \dot{x}_3(0) = 0$, and the parameter values of the control input (2) are: $x_{ref} = 3$ $[mm]$, and $\alpha_1 = \alpha_2 = 10.187$ $\left[\frac{1}{\mathrm{s}}\right]$. In Figures 3a and 3b, x_{ref} and its negative counterpart are indicated by two horizontal black dotted lines.

As becomes clear from Figure 3a, although the oscillators are released close to anti-phase synchronization, in steady-state the oscillators synchronize in-phase as depicted in Figures 3b and 3d. Additionally, Figure 3c shows the projection of the displacements of the two oscillators onto the plane (x_1,x_2). The black part of the curve corresponds to the transient behaviour prior to reach the in-phase steady-state part of the curve indicated in grey.

The behaviour of the coupling bar is depicted in Figure 5a. Initially, the displacement of the bar is very small due to the anti-phase like start-up. When the phase difference between the oscillators converges to zero, the oscillation corresponding to the displacement of the bar increases until the oscillators synchronize in-phase. Then, the bar keeps oscillating with fixed frequency and amplitude.

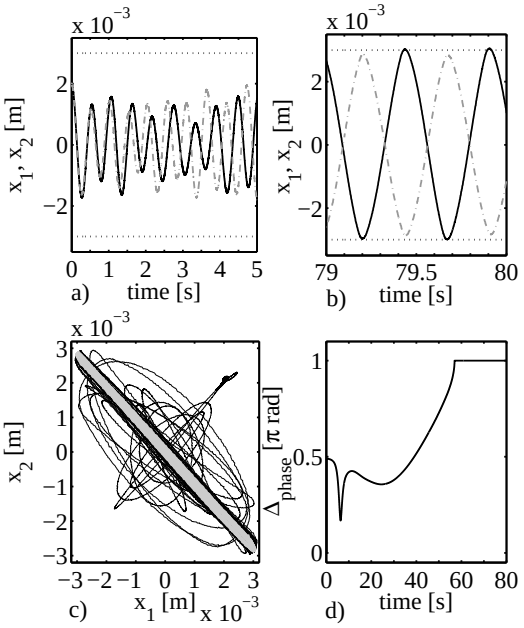

Figure 4. In this experiment, the oscillators synchronize in anti-phase (in figures a) and b) solid line: x_1, dashed-dotted line: x_2).

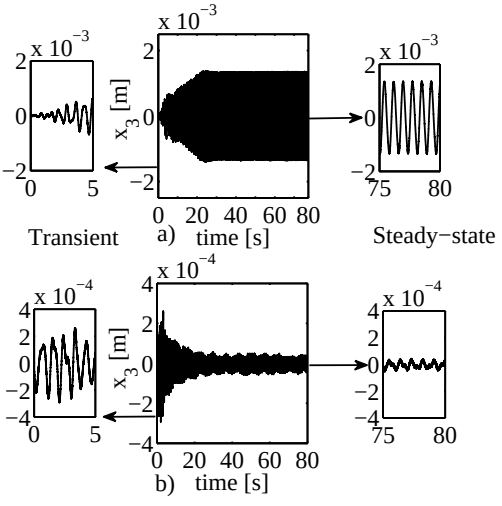

Figure 5. Displacement of the bar when the oscillators synchronize: a) in-phase, b) in anti-phase.

In a second experiment, the mass of the coupling bar is increased by adding two steel plates of 2.359 [kg] each. This yields $m_3 = 8.818$ [kg]. Note that with this value of m_3 and assuming parameter values as given in Table 1, the conditions for Proposition 1 are fulfilled and anti-phase steady-state motion is likely to occur. As depicted in Figure 4a, the oscillators are released from initial conditions close to in-phase, $x_1(0) = 1.97$ $[mm]$, $\dot{x}_1(0) = 0$, $x_2(0) = 2.13$ $[mm]$, $\dot{x}_2(0) = 0$, and $x_3(0) = \dot{x}_3(0) = 0$. After the transient behaviour, the oscillators synchronize in anti-phase as can be seen in Figures 4b and 4d. In this case, Proposition 1 is only applicable for $t < t_1 = 21.6$ $[s]$, where t_1 is the time, at which $|x_i| = x_{ref}$ for the first time, and the behaviour becomes nonlinear. Figure 4c shows the projection of the displacements corresponding to the oscillators onto the plane (x_1,x_2). Again, the black part of the curve corresponds to the transient behaviour prior to reach the steady-state anti-phase indicated by the grey part of the curve. Ideally, the displacement of the coupling bar should go to zero. However, due to the fact that the amplitudes of the oscillators differ slightly, because in the experimental setup the oscillators are not completely identical, the coupling bar does not come to a complete standstill as depicted in Figure 5b. Nevertheless, the phase difference between the oscillators is approximately π [rad] as depicted in Figure 4d. As a matter of fact, the anti-phase synchronized motion observed in this experiment can also be seen if the oscillators are released from the same initial conditions as used in experiment 1.

For the next experiments, the energy-based controller (8) is applied to the oscillators. The suspended bar is again allowed to oscillate freely and the experiments are carried out by using the same parameter values presented in Table 1.

In the first experiment, no extra mass is added to the coupling bar, hence $m_3 = 4.1$ [kg]. The oscillators are released from the initial conditions $x_1(0) = 2.7$ $[mm]$, $x_2(0) = -2.9$ $[mm]$, $\dot{x}_1(0) = \dot{x}_2(0) = x_3(0) = \dot{x}_3(0) = 0$. The parameters in controller (8) are taken to be $\lambda = 2.907{\cdot}10^3$, $\kappa = 37.108$ $\left[\frac{\mathrm{N}}{\mathrm{m}}\right]$, and $x_{ref} = 6.5$ $[mm]$.

The oscillators are released close to anti-phase sync, as depicted in Figure 6. Nevertheless, in steady-state the system synchronizes in-phase. Additionally, Figure 6 shows that in steady-state the amplitudes corresponding to the displacements x_1, x_2 are approximately equal and the phase difference between the oscillators is 0 rad.

Initially, the displacement of the bar, i.e. x_3, is very small due to the anti-phase start-up. When one of the oscillators decreases its amplitude, the oscillation corresponding to the bar displacement increases until the moment the oscillators synchronize in-phase. After that, the bar keeps oscillating with a fixed frequency and amplitude as depicted in Figure 6c.

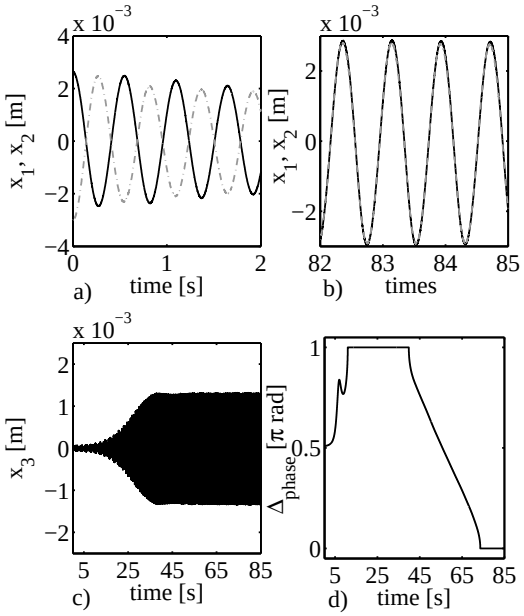

Figure 6. Experimental results. In-phase synchronization occurs for $m_3 = 4.1$ [kg] (in figures a) and b) solid line: x_1, dashed-dotted line: x_2).

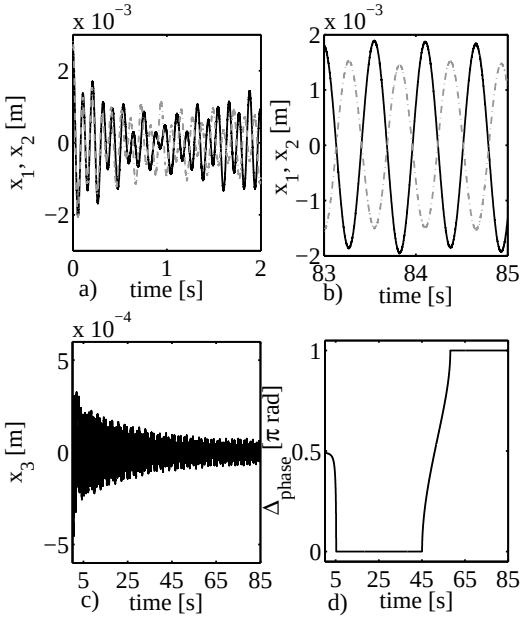

Figure 7. The mass of the coupling bar is increased to $m_3 = 8.818$ [kg]. As a consequence, the oscillators synchronize in anti-phase (in figures a) and b) solid line: x_1, dashed-dotted line: x_2).

In a second experiment, the mass of the coupling bar is increased by again adding two steel plates of 2.359 [kg] each. This again yields $m_3 = 8.818$ [kg]. The oscillators are released from initial conditions close to in-phase, $x_1(0) = 2.7$ $[mm]$, $\dot{x}_1(0) = 0$, $x_2(0) = 2.9$ $[mm]$, $\dot{x}_2(0) = 0$, and $x_3(0) = \dot{x}_3(0) = 0$. In this

case, the system synchronizes in anti-phase as can be seen in Figure 7. Ideally, the displacement of the coupling bar denoted as x_3 should go to zero. However, due to the fact that the amplitudes of the oscillators, denoted as x_1 and x_2, differ by a factor 1.2, the coupling bar does not come to a complete standstill as depicted in Figure 7c. Nevertheless, the phase difference between the oscillators is approximately π rad as depicted in Figures 7b and 7d.

These experimental results show that when the system synchronizes in anti-phase, the oscillation frequency is approximately the same as the natural frequency of the oscillators, whereas for the in-phase synchronization case, the oscillation frequency is approximately the same as the natural frequency of the coupling bar.

4 Synchronization of two coupled van der Pol oscillators

In this section, the synchronization of two van der Pol oscillators is analyzed.

Consider the mechanical system of Figure 1 with $U_i = 0$ $(i = 1, 2, 3)$, and damping characteristic

$$\beta_i(q_i) = \lambda \left(a q_i^2 - 1\right), \quad i = 1, 2, \tag{13}$$

where $q_i = x_i - x_3$, $\lambda \in \mathbb{R}^+$, and $a \in \mathbb{R}^+$. Then, the equations of motion are

$$\begin{aligned} m_1\ddot{x}_1 &= -\kappa_1(x_1 - x_3) - \beta_1(q_1)(\dot{x}_1 - \dot{x}_3) \\ m_2\ddot{x}_2 &= -\kappa_2(x_2 - x_3) - \beta_2(q_2)(\dot{x}_2 - \dot{x}_3) \\ m_3\ddot{x}_3 &= -\sum_{i=1}^{2} m_i\ddot{x}_i - \kappa_3\dot{x}_3 - \beta_3\dot{x}_3. \end{aligned} \tag{14}$$

The system under consideration represents two van der Pol oscillators coupled through a movable support. It is possible to show that system (14) has two invariant manifolds [Belykh et al., 2008]:

$$M_{in} := \{(x_1, \dot{x}_1) = (x_2, \dot{x}_2)\}, \tag{15}$$

$$M_{anti} := \{(x_1, \dot{x}_1) = (-x_2, -\dot{x}_2), \quad x_3 = \dot{x}_3 = 0\}. \tag{16}$$

Therefore, system (14) has at least two possible limit behaviours, namely in-phase and anti-phase synchronization.

Moreover, the limit synchronizing behaviour can not only be influenced by the masses of the oscillators relative to the mass of the coupling bar as will be shown later, but also by the initial conditions as depicted in Figure 8, which has been obtained by computer simulations. For this analysis, all parameter values of system (14) were fixed to the values given in Table 3 with $\lambda = 3$, and $a = 1.8 \times 10^5$. Only the initial conditions were varied. Moreover, it should be noted that only part of the initial conditions is varied here. All other initial conditions are zero. In the plot, black points represent initial conditions that go to anti-phase $e = (x_1 + x_2) = 0$, while red points represent initial conditions that go to in-phase $e = (x_1 - x_2) = 0$.

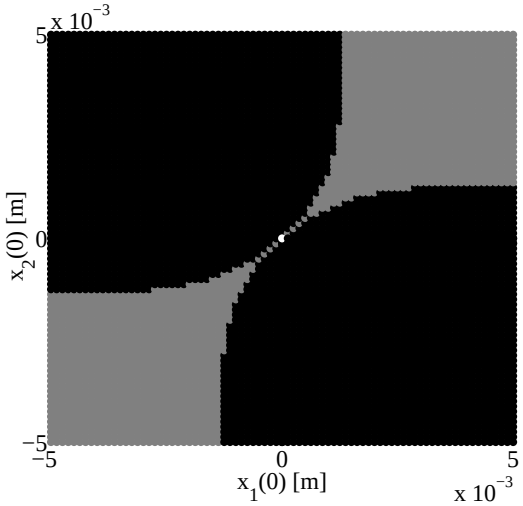

Figure 8. Projection of the limit behaviour onto the (x_1, x_2) plane for a set of fixed parameters. Black points represent initial conditions that go to anti-phase $e = (x_1 + x_2) = 0$, while red points represent initial conditions that go to in-phase $e = (x_1 - x_2) = 0$.

4.1 Adjustment of the experimental setup to mimic the van der Pol oscillators

The adjustment of the setup of Figure 1 is made by using feedback control. This requires to design suitable controllers $U_i,\ i = 1, 2, 3$. First, cancellation of a part of the original dynamics (1) and secondly, enforcement of the dynamics (14) corresponding to two coupled van der Pol oscillators is required. The cancellation part is achieved by using an approximated model obtained by parametric identification in combination with a robust observer [van den Elshout, 2010; Rosas, Alvarez, Fridman (2006)]. This observer reconstructs the state vector, since in the experimental setup only positions are measured.

The experimental setup depicted in Figure 1 is adjusted to mimic system (14) by defining the actuator forces of system (1) as follows

$$\begin{aligned} U_i = m_i &\left(\omega_i^2(x_i - x_3) + 2\zeta_i\omega_i(\dot{x}_i - \dot{x}_3)\right) \\ &-\kappa_i(x_i - x_3) - \beta_i(q_i)(\dot{x}_i - \dot{x}_3),\ i = 1, 2, \end{aligned} \tag{17}$$

$$\begin{aligned} U_3 = m_3 &\left(\omega_3^2 x_3 + 2\zeta_3\omega_3\dot{x}_3 - \psi(\cdot)\right) - \kappa_3 x_3 - \beta_3\dot{x}_3 \\ &+ \sum_{i=1}^{2} \left[\kappa_i(x_i - x_3) + \beta_i(q_i)(\dot{x}_i - \dot{x}_3)\right]. \end{aligned} \tag{18}$$

where $\psi(\cdot) = \sum_{i=1}^{2} \mu_i \left[\frac{\kappa_i}{m_i}(x_i - x_3) + \frac{\beta_i(q_i)}{m_i}(\dot{x}_i - \dot{x}_3)\right]$.

	Osc. 1	Osc. 2	Coupling bar
ω_i [rad/s]	12.5521	14.0337	9.7369
ζ_i $[-]$	0.3362	0.4226	0.0409
m_i [kg]	0.198	0.210	4.1

Table 2. Parameters values for the experiments according to model (1).

	Osc. 1	Osc. 2	Coupling bar
$\kappa_i \left[\frac{\mathrm{N}}{\mathrm{m}}\right]$	37.108	37.108	388.71
m_i [kg]	1.210	1.210	4.1

Table 3. Parameters values for the experiments according to model (14).

In closed-loop, the dynamics of system (1) with controllers (17)-(18) coincide with dynamics (14).

4.2 Experimental results

The experimental setup of Figure 1 is used in order to experimentally investigate the synchronizing behaviour of two coupled van der Pol oscillators.

Hence, we consider model (1) with parameter values given in Table 2 and controls (17)-(18) with parameter values given in Table 3 except that $m_1 = m_2 = 1$ [kg], and $\lambda = 0.1$, $a = 1.8 \times 10^5$.

In a first experiment, the oscillators are released from the initial conditions $x_1(0) = 4.9$ [mm], $x_2(0) = 4.8$ [mm]. The remaining initial conditions are taken to be zero.

Although the oscillators are released close to in-phase motion, as depicted in Figure 9a, the system converges to the anti-phase manifold (16) as becomes clear from Figure 9b and as a consequence the oscillations in the coupling bar decay as shown in Figure 9c. Indeed, the anti-phase synchronization of the coupled van der Pol oscillators is illustrated further by projecting the displacements corresponding to the oscillators in the plane (x_1, x_2) as depicted in Figure 9d. The dark grey part of the curve corresponds to the initial in-phase motion whereas the light grey corresponds to the transient behaviour prior to reach the anti-phase part of the curve indicated in black.

In a second experiment, the oscillators are released from initial conditions close to anti-phase motion, i.e. $x_1(0) = -4.9$ [mm] and $x_2(0) = 4.8$ [mm], as depicted in Figure 10a. The remaining initial conditions are taken to be zero. The masses of the oscillators, corresponding to the virtual system (14), are decreased such that $m_1 = m_2 = 0.210$ [kg] and the value of the parameter λ is increased to $\lambda = 3$. As a result, the van der Pol oscillators converge to the in-phase manifold (15), as depicted in Figure 10b. The coupling bar, which is initially at rest, starts moving until it reaches an oscillation with constant amplitude and frequency as

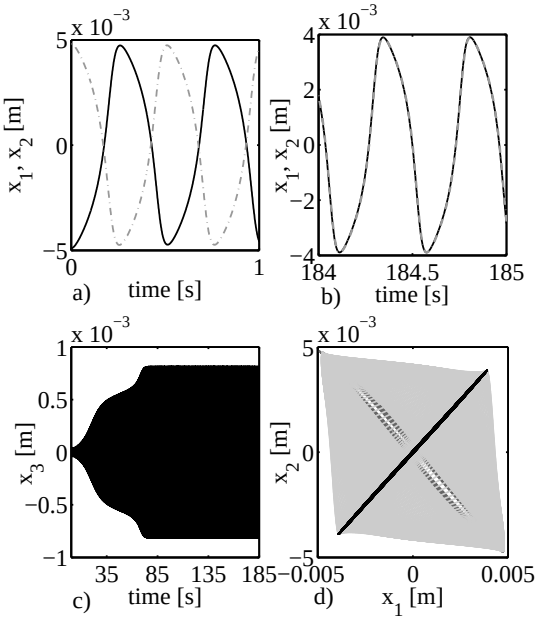

Figure 9. Experiment in which two coupled van der Pol oscillators synchronize in anti-phase (in figures a) and b) solid line: x_1, dashed-dotted line: x_2).

depicted in Figure 10c. The steady-state behaviour is illustrated further by projecting the displacements corresponding to the oscillators in the plane (x_1, x_2) as depicted in Figure 10d. The initial behaviour, is denoted by the dark grey part of the curve whereas the steady-state behaviour is represented by the black part of the curve. Clearly, the van der Pol oscillators are synchronized in-phase.

5 Conclusions and recommendations

Experimental analyses related to the phase synchronization occurring in nonlinear oscillators with Huygens' coupling have been presented. For the case of two mass-spring-damper oscillators, two types of controllers have been considered. It has been shown that the coupling strength (the ratio between the mass of the oscillators and the mass of the bar) influences the onset of in-phase and anti-phase synchronization. Moreover, the synchronized motion in the oscillator is independent of the kind of controller used to resupply energy into the system. Additionally, by using state feedback, the dynamics of our experimental setup has been converted to the dynamics of two van der Pol oscillators. In this case, the limit synchronizing behaviour not only depends on the coupling strength but also on the initial conditions. In summary, Huygens' coupling seems to generalize the synchronized phenomenon in the sense that not only pendulum clocks but also other arbitrary second order oscillators may spontaneously synchronize. With respect to the presented synchronization results, it is still necessary to carry out a complete and rigorous nonlinear stability analysis.

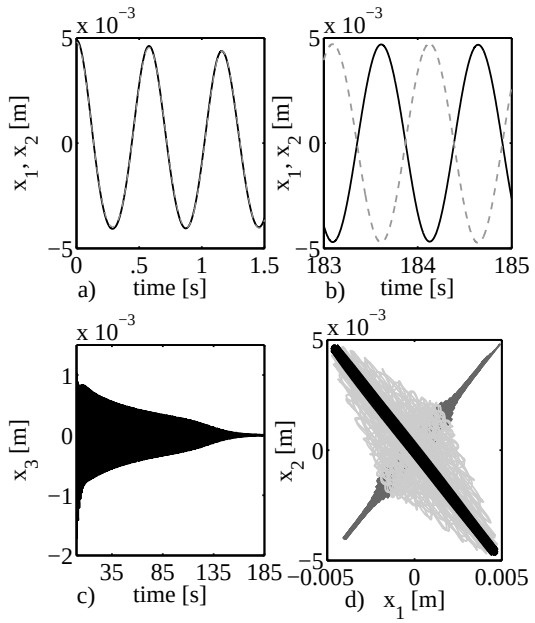

Figure 10. In this experiment the van der Pol oscillators synchronize in-phase (in figures a) and b) solid line: x_1, dashed-dotted line: x_2).

6 Acknowledgments

The first author acknowledges the support of the Mexican Council for Science and Technology (CONACYT).

References

Belykh, V.N., Pankratova, E.V., Pogromsky, A.Yu., and Nijmeijer, H. (2008) Two van der Pol-Duffing oscillators with Huygens coupling. In *Proceedings of the 6th EUROMECH Nonlinear Dynamics Conference, Saint Petersburg, Russia.*

Bennett, M., Schatz, M., Rockwood, H., and Wiesenfeld, K. (2002) Huygens' clocks. *Proceedings of the Royal Society of London A: Mathematical, Physical and Engineering Sciences*, **458**(2019), pp. 563–579.

Blekhman, I. (1988) *Synchronization in science and technology*. ASME Press, New York.

Czolczynski, K., Perlikowski, P., Stefansky, A., and Kapitaniak (2011) Huygens' odd sympathy experiment revisited. *International Journal of Bifurcation and Chaos*, **12**(7), pp. 2047–2056.

Dilão, R. (2009) Antiphase and in-phase synchronization of nonlinear oscillators: The Huygens's clocks system. *Chaos: An Interdisciplinary Journal of Nonlinear Science*. **19**(2), pp. 023118–023118-5.

Huygens, C. (1660). *Oeuvres completes de Christiaan Huygens*. M. Nijhoff (ed.), **17**, pp. 156–189.

Oud, W.T., Nijmeijer, H., and Pogromsky, A.Yu. (2006) A study of Huijgens synchronization: experimental results. In *Group Coordination and Cooperative Control. Lecture Notes in Control and Information Sciences*, Pettersen, K., Gravdahl, J., Nijmeijer, H. (eds.), Springer, Berlin. **336**, pp. 191–203.

Pantaleone, J. (2002) Synchronization of metronomes. *American Journal of Physics*, **70**(10), pp. 992–1000.

Pena-Ramirez, J., Fey, R.H.B., and Nijmeijer, H. (2011) An experimental study on synchronization of nonlinear oscillators with Huygens' coupling. *Nonlinear Theory and its Applications, IEICE*, **E95-N**(4).

Pikovsky, A., Rosenblum, M., and Kurths, J. (2001) *Synchronization. A Universal Concept in Nonlinear Sciences*. Cambridge University Press, Cambridge.

Pogromsky, A.Yu., Belykh, V.N. and Nijmeijer, H. (2003) Controlled synchronization of pendula. In *Proceedings 42nd IEEE International Conference on Decision and Control, December 9-12, Maui, Hawaii, USA.* **5**, pp. 4381–4386.

Rayleigh, J. (1945) *Theory of Sound*. Dover, New York.

Rosas, D., Alvarez, J., and Fridman, L. (2006) Robust observation and identification of nDOF Lagrangian systems. *International Journal of Robust and Nonlinear Control*, **17**, pp. 842–861.

Strogatz, S. (2003) *Sync: the emerging science of spontaneous order*. Hyperon, New York.

van den Elshout, B. (2010) *Implementation of self-synchronizing Huijgens' pendula*. Master thesis. Dynamics and Control Group. Department of Mechanical Engineering. Eindhoven University of Technology.

van der Pol, B. (1920) Theory of the amplitude of free and forced triode vibration. *Radio Review*, **1**, pp. 701–710.